Difficulties in Choosing Sine-Wave Filter Capacitances and Inductances

MIKHAIL PUSTOVETOV
Department of Electrical and Electronics Engineering
Don State Technical University
344000, Rostov region, Rostov-on-Don, Gagarin sq., 1
RUSSIA

Abstract: Relevance of the work reflects the increased use in practice of variable frequency electric drive additional options, which include sine-wave filter. It is shown that due to the presence of a gain band in the Bode magnitude diagram of a sine-wave filter, some undesirable voltage harmonics are amplified regardless of the choice of parameters. Designs of magnetic cores of inductors in the filter are recommended, which help suppress not only differential-mode, but common-mode components of voltage and current too.

Key-Words: sine-wave filter, semiconductor frequency converter, resonant frequency, capacitance, inductance, magnetic core, common-mode interference, differential-mode interference

Received: May 8, 2024. Revised: March 6, 2025. Accepted: April 9, 2025. Published: May 19, 2025.

1 Introduction

A sine-wave filter (SF) is currently a widely used component of electrical circuits containing pulse voltage sources, such as frequency converters (FC) [1], [2], [3], [4], [5]. The electrical circuit diagram of the SF, its purpose, properties, and application are described in [6]. The SF ensures electromagnetic compatibility of the FC and the load, such as an AC motor. When analyzing the parameters of serially produced SF [7], [8], [9], it becomes clear that an important requirement for design is the value of the fundamental harmonic voltage drop across the inductor of the SF at rated current (impedance), which in most cases does not exceed 10% of the load rated RMS phase voltage. That is, having selected the inductance of the SF [10], then the SF capacitance is calculated based on the resonant frequency f_{rez}, which for the SF should be higher than the highest frequency of the fundamental harmonic, but lower than the carrier frequency of the pulse-width modulation (PWM). Another approach to determining the SF parameters is possible, demonstrated by the authors of [11] based on Appendix E [12]. In this case, the attenuation at the switching frequency and the minimum damping factor are specified. A variable voltage variable frequency electric drive, by deliberately changing the frequency f_1 of the fundamental harmonic of the voltage at the FC output, allows for the formation of starting and braking modes of the AC motor, and also ensures its operation in a wide range of rotation speeds. A property of the SF is the impossibility of ensuring the same quality (THD [13]) of the output voltage in the entire f_1 range. This is due to the presence of a maximum (peak gain of the output voltage relative to the input voltage) in the Bode magnitude diagram of SF at f_{rez}.

2 Possible Increase of Torque Ripple in a Variable Voltage Variable Frequency Drive

Let us have a FC with a control range of $f_1 = 0...50$ Hz, equipped with a SF with $f_{rez} = 195$ Hz. The PWM carrier frequency of the FC is $f_{PWM} = 1000$ Hz. The frequencies of higher harmonics of voltage can coincide with f_{rez} at some values of f_1 (see Table 1). In this case, the shape of the voltage at the output of the SF is distorted by oscillations at a frequency close to f_{rez}. The effect of the distorted voltage sinusoid is not limited to an increase in losses in the elements of the electrical circuit. Harmonics of the supply voltage cause ripple of the air-gap torque of AC motor, for example, the case for a three-phase induction motor (see Table 1) is described in [14], [15]. Having obtained an amplification of some voltage harmonics after the SF, it becomes possible to obtain air-gap torque ripples magnitudes at some frequencies higher than would be the case without the SF.

Fig. 1 shows vectors $\overrightarrow{AB}$ and $\overrightarrow{AC}$ rotating in the same direction with the same angular frequency $6 \cdot \omega_1 \cdot t$, the projections of each of which on the Torque axis symbolize, respectively, the synchronous torques from the interaction of the 1st harmonic of induction and the 5th time harmonic of the rotor current T_{1_5} and the 1st harmonic of induction and the 7th time harmonic of the rotor current T_{1_7}. Vector $\overrightarrow{AD}$ is the sum of vectors $\overrightarrow{AB}$ and $\overrightarrow{AC}$, and its projection on the Torque axis symbolizes the pulsating torque formed by the joint action of T_{1_5} and T_{1_7} [14], [15].

Table. 1 Situations when the maximum gain of individual higher harmonics of the voltage at the output of the SF is achieved

Frequency of fundamental harmonic of voltage f_1, Hz	The order of the voltage harmonic coinciding with $f_{rez} = 195$ Hz	Air-gap torque ripple's frequency for AC motor, Hz
39.0	5th	$f_T = 6 f_1 = 234.0$
27.9	7th	$f_T = 6 f_1 = 167.4$
17.7	11th	$f_T = 12 f_1 = 212.4$
15.0	13th	$f_T = 12 f_1 = 180.0$

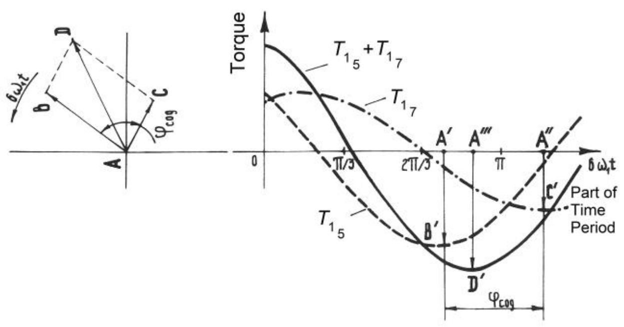

Figure 1 - Interference in time of coherent waves of air gap torque

Thus, both components of the torque are coherent waves and have the ability to interfere in time. In other words, the result of adding two simple harmonic oscillations of the same frequency is a simple harmonic oscillation of the same frequency.

3 Problems of Voltage Waveform Provision During Equipment Testing

When testing transformers (T), open circuit or no load and short-circuit (SC) or impedance tests are carried out, during which it is necessary to supply alternating voltage of an approximately sinusoidal shape with a rated frequency to the tested T [16]. FCs are used as adjustable power supplies when testing electrical equipment [17]. In order to overcome the contradiction between the pulse shape of the FC output voltage, formed according to the PWM principle, and the need to supply sinusoidal voltage to the tested T, a SF is connected to the FC output.

Let's consider a specific situation. There is a FC with a rated apparent power of $S_{2rated} = 1$ MVA. The design feature of this FC is that it consists of two identical converters (the rated apparent power of each is $S_{1rated} = 500$ kVA) whose output voltages are precisely synchronized. The RMS value of the rated line voltage at the FC's input is $V_{lineIN} = 690$ V. The same value can be obtained at the FC's output: $V_{lineOUT} = 690$ V. The frequency of the fundamental harmonic of the voltage at the FC's output can be adjusted up to $f_1 = 200$ Hz. The FC is assumed to be used at output frequencies from 50 Hz to 200 Hz. The preset carrier frequency of PWM is $f_{PWM} = 2000$ Hz [17].

Let's consider an example of the load that the FC operates on. In our case, this is a powerful T of the TM-1000/10-76T1 type in the SC test mode. The SC test losses for this type of T are $p_{SC} = 10800$ W. The SC test is carried out at the rated phase current of the high-voltage side (the windings are connected in a Δ) $I_{PHrated} = 57.7$ A. The SC test voltage of T is 7.25%. At the RMS rated voltage of T of 10,000 V, this will be $V_{SC} = 725$ V.

Equivalent resistance of T

$$r_{eq\Delta} = \frac{p_{SC}}{3 \cdot I_{PHrated}^2} = \frac{10800}{3 \cdot 57.7^2} = 1.081 \text{ Ohm.}$$

Phase current in a SC test conducted at a line voltage $V'_{SC} = V_{lineOUT} = 690$ V

$$I'_{PH} = \frac{V'_{SC}}{V_{SC}} \cdot I_{PHrated} = \frac{690}{725} \cdot 57.7 = 54.9 \text{ A}.$$

The SC test losses at RMS current $I'_{PH} = 54.9$ A

$$p'_{SC} = 3 \cdot {I'_{PH}}^2 \cdot r_{eq\Delta} = 3 \cdot 54.9^2 \cdot 1.081 = 9782.4 \text{ W}.$$

True component of SC test voltage at $I'_{PH} = 54.9$ A

$$V'_{SCt} = I'_{PH} \cdot r_{eq\Delta} = 54.9 \cdot 1.081 = 59.4 \text{ V}.$$

Reactive component of SC test voltage at $I'_{PH} = 54.9$ A

$$V'_{SCr} = \sqrt{V'^2_{SC} - {V'_{SCt}}^2} = \\ = \sqrt{690^2 - 59.4^2} = 687.4 \text{ V}.$$

Equivalent reactance of T

$$x_{eq\Delta} = \frac{V'_{SCr}}{I'_{PH}} = \frac{687.4}{54.9} = 12.518 \text{ Ohm}.$$

Equivalent inductance of T

$$L_{eq\Delta} = \frac{x_{eq\Delta}}{2 \cdot \pi \cdot f_1} = \frac{12.518}{2 \cdot \pi \cdot 50} = 0.0399 \text{ H}.$$

Reactive power per phase in SC test at $V'_{CS} = 690$ V

$$Q'_{SCPH} = {I'_{PH}}^2 \cdot x_{eq\Delta} = \\ = 54.9^2 \cdot 12.518 = 37750.4 \text{ var}.$$

Total reactive power of the load in SC test at $V'_{CS} = 690$ V

$$Q'_{SC} = 3 \cdot Q'_{SCPH} = \\ = 3 \cdot 37750.4 = 113251.3 \text{ var}.$$

The total load apparent power in SC test mode at an RMS line voltage of 690 V will be

$$S'_{SC} = \sqrt{{p'_{SC}}^2 + {Q'_{SC}}^2} = \\ \sqrt{9782.4^2 + 113251.3^2} = 113673 \text{ VA},$$

which is 11.4% of the rated apparent power of the FC.

The value of the capacitance per phase when connecting capacitances in a Δ configuration, which completely compensates for the reactive power of the load (T in the SC test)

$$C_\Delta = \frac{Q_{SC}}{2 \cdot \pi \cdot f_1 \cdot V'^2_{SC}} = \frac{37750.4}{2 \cdot \pi \cdot 50 \cdot 690^2} = 252.5$$

μF.

The value of the capacitance per phase when connecting the capacitances according to the Y scheme, completely compensating the reactive power of T in the SC test

$$C_Y = 3 \cdot C_\Delta = 3 \cdot 252.5 = 757.6 \text{ μF}.$$

If we consider half of T as the load for one half of the FC, then it will bear: half of the SC test losses, half of the SC test reactive power; half of the SC test current. This will lead to a twofold increase in the resistance and inductance of the load, as well as a twofold decrease in the calculated values of the capacitance, which fully compensates for the reactive power of the load: $C_{1\Delta} = 126.3$ μF; $C_{1Y} = 378.8$ μF.

The SF, connected at the FC output, is also composite. Half of the SF is connected to the output of each of the FC's halves, containing a reactor with an inductance of $L_1 = 0,2$ mH in each phase and a parallel connection of two capacitors of 60 μF, which gives a capacitance of $C_{1\Delta} = 120$ μF. Capacitances of 120 μF are connected in a Δ configuration. Such a connection is equivalent to a Y connection of $C_{1Y} = 3 \cdot C_{1\Delta} = 120 \cdot 3 = 360$ μF capacitances. The outputs of the same phases of the SF halves are connected to each other. That is, the SF halves are connected in parallel to each other, which for the complete SF gives the following parameters: $L = L_1 / 2 = 0.2 / 2 = 0.1$ mH; $C_\Delta = C_{1\Delta} \cdot 2 = 120 \cdot 2 = 240$ μF; $C_Y = C_\Delta \cdot 3 = 240 \cdot 3 = 720$ μF. Also, at the output of each FC's half, additional reactors with an inductance of 0.032 mH per phase are connected in series with the SF inductances. The results of the SF characteristics calculations are summarized in Table 2. From Table 2 it follows that it does not matter whether we consider the complete SF or its half. Let us construct the Bode magnitude diagram for four sets of SF parameters for the complete SF specified in Table 3.

Among the products of the Schaffner company there are SFs for V with residual voltage pulsations of less than 5%. The frequency of the fundamental harmonic of the voltage at the FC output can be adjusted up to 200 Hz. The phase capacitors are connected according to the Y scheme. The parameters published in [18] for the Schaffner SF are given in Table 4. SF FN 5040 HV-940-99 from Table 4 was taken as Set #2 in Table 3.

The results of constructing the Bode magnitude diagrams for four sets of SF parameters, including the voltage gain factor at the SF output relative to the input $GF = V_{SFout} / V_{SFin}$, are summarized in Table 5.

In the case of parameter set #4, we have $C_{1\Delta} = 1200$ μF (Fig. 2, Fig. 3). When equipping each half of the FC with such a capacitance, the reactive power of the inductive load of 1.137 Mvar can be compensated, which seems excessive.

Table. 2 Calculated characteristics of the SF

Complete SF	Half of SF
Resonant frequency, Hz	
$f_{rez} = \dfrac{1}{2\pi\sqrt{L_L \cdot C_Y}} = \dfrac{1}{2\pi\sqrt{0.1 \cdot 10^{-3}}} \times \dfrac{1}{\sqrt{720 \cdot 10^{-6}}} = 593.136$	$f_{1rez} = \dfrac{1}{2\pi\sqrt{L_{1L} \cdot C_{1Y}}} = \dfrac{1}{2\pi\sqrt{0.2 \cdot 10^{-3}}} \times \dfrac{1}{\sqrt{360 \cdot 10^{-6}}} = 593.136$
Rated current of the FC, assuming the load is connected in a Y configuration, A	
$I_{Lrated} = \dfrac{S_{2rated}}{3 \cdot \dfrac{V_{lineOUT}}{\sqrt{3}}} = \dfrac{S_{2rated}}{\sqrt{3} \cdot V_{lineOUT}} = \dfrac{1000000}{\sqrt{3} \cdot 690} = 836.74$	$I_{L1rated} = \dfrac{I_{Lrated}}{2} = \dfrac{836.74}{2} = 418.37$
Voltage drop across the inductor at 50 Hz as a percentage of the rated phase voltage $V_{phOUT} = \dfrac{V_{lineOUT}}{\sqrt{3}} = \dfrac{690}{\sqrt{3}} = 398.37$ V	
$\Delta V_{L\%} = \dfrac{2\pi \cdot f_1 \cdot L \cdot I_{Lrated}}{V_{phOUT}} \times 100\% = 2\pi \cdot 50 \cdot 0.1 \cdot 10^{-3} \cdot 836.74 \cdot 100\% / 398.37 = 6.6\%$	$\Delta V_{1L\%} = \dfrac{2\pi \cdot f_1 \cdot L_1}{V_{phOUT}} \times I_{L1rated} \cdot 100\% = 2\pi \times 50 \cdot 0.2 \cdot 10^{-3} \times 418.37 \cdot 100\% / 398.37 = 6.6\%$

Table. 3 Sets of SF parameters (for two halves of the SF in total)

Set #	1	2*	3	4
L, mH	0.1 + 0.016	0.16	0.1 + 0.016	0.1 + 0.016
C_Y, μF	720	612	240	7200
I_{Lrated}, A	836.74	940	836.74	836.74
$\Delta V_{L\%}$	6.6	11.85	6.6	6.6
f_{PWM}, Hz	2000	Not more than 1500	2000	2000

*Set #2 is SF of type Schaffner FN 5040 HV-940-99

Table. 4 Parameters and characteristics of the Schaffner SF @ $V_{lineOUT} = 690$ V according to [18]

SF type	FN 5040 HV-430-99	FN 5040 HV-940-99
L, mH	0.35	0.16
C_Y, μF	272	616
I_{Lrated}, A	430	940
f_{rez}, Hz	515.8	508.6
$\Delta V_{L\%}$	11.86	11.85
Minimal f_{PWM}, Hz	1500	1500

Table. 5 Results of constructing the Bode magnitude diagrams

Set #	$f_{\text{рез}}$, Hz / GF @ $f_1 = 50$ Hz	GF @ the gain band boundaries, Hz	The gain band includes harmonics of orders $f_1 = 50$ Hz	Note
1	549.5	272÷733	7th (350 Hz); 11th (550 Hz); 13th (650 Hz)	Disadvantage: 11th harmonic @ $f_1 = 50$ Hz coincided with the resonant frequency
	1.0			

2	508.6 0.998	251÷ 676		Disadvantages: 1) 5th harmonic @ $f_1 = 102$ Hz coincided with the resonant frequency; 2) 7th harmonic at $f_1 = 73$ Hz coincided with the resonant frequency
3	955.0 0.994	463÷1270	11th (550 Hz); 13th (650 Hz); 17th (850 Hz); 19th (950 Hz); 23rd (1150 Hz); 25th (1250 Hz)	Disadvantages: 1) The 19th harmonic @ $f_1 = 50$ Hz is close to the resonant frequency; 2) amplification of six harmonics at once, which is to some extent compensated for by the high frequency of these harmonics
4 (see Fig. 2)	173.8	86 ÷232	See Fig. 3. 3rd (150 Hz) (if used for PWM generation)	Advantages: almost all higher harmonics are suppressed in the entire range of 50 ... 200 Hz of the fundamental frequency of the FC. Disadvantages: 1) the 3rd harmonic @ $f_1 = 58$ Hz coincides with
	1.08			the resonant frequency; 2) @ $f_1 > 88$ Hz there is a significant amplification of the fundamental voltage harmonic; 3) the reactive power of the SF capacitors is excessive to compensate for the inductive power of the load, which can lead to unacceptably high currents through the semiconductor switches of the FC [3].

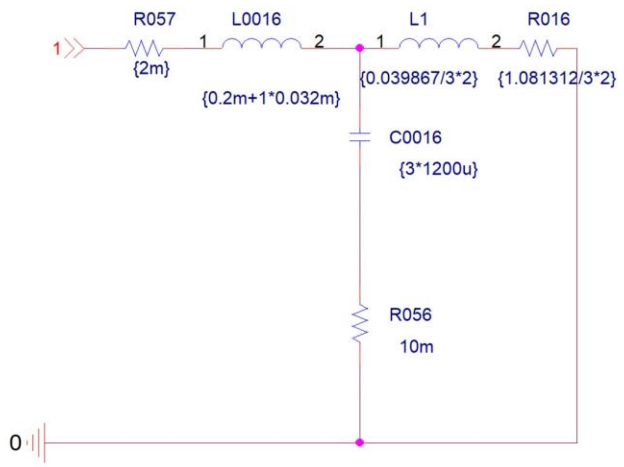

Figure 2 - Circuit for computer simulation of the Bode magnitude diagram of the phase of the SF loaded on the T of type TM-1000/10-76T1 in the SC test mode (set of parameters # 4 according to Table 1). The parameters in the circuit are set in such a way that it is assumed, that half of the SF is simulated with Y connection scheme of the phases of the SF capacitances and the load phases (the resistance delta is transformed into an equivalent wye)

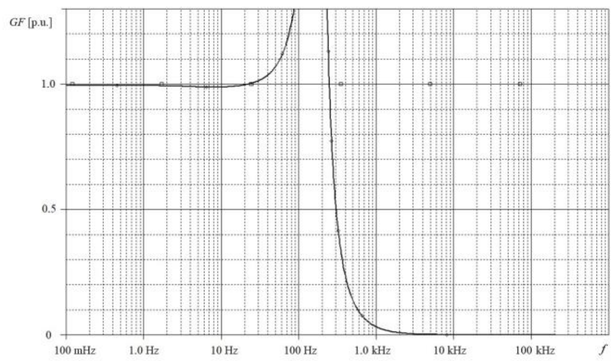

Figure 3 - Bode magnitude diagram (results of circuit simulation according to Fig. 2) for a SF with $C_{1\Delta} = 1200$ μF and $L_1 = 0.2$ mH taking into account the presence of an additional 0.032 mH inductive reactor at the FC output (set of parameters # 4 according to Table 1)

None of the four sets of considered parameters of the SF allows to avoid amplification of one or another higher harmonic (in most cases several harmonics) or even the first harmonic at the upper end of the voltage frequency regulation range. Therefore, without resorting to excessive increase in the capacitance of the SF capacitors [3] (set of parameters # 4), it is necessary to choose the option in which the distortion of the voltage shape at the SF output will be minimal in the required range of change of the fundamental frequency of the FC. A separate question is whether the quality of the voltage at the SF output will satisfy the requirements imposed by the load [16], [17].

4 The Problem of Zero-Sequence Currents

According to [6], SFs are used to suppress antiphase voltage components (differential-mode interference according to the terminology of [19]), but are ineffective for suppressing zero-sequence components (common-mode interference [19]). When powering an AC motor from an FC, one of the problems is damage to bearings by leakage zero-sequence currents [20], [21], [22] which arise due to the presence of zero-sequence components in the FC output voltage spectrum, i.e. common-mode (caused by the switching algorithms of the FC transistors).

In [6], for complex suppression of both differential and common-mode components of the voltage at the FC output, it is recommended to use a sine-wave filter and a dv/dt filter connected in series [23], [24]. In this case, the dv/dt filter must contain a common-mode inductive reactor. Such an approach is implemented, for example, in SineFormer devices from TDK and EPCOS [25], [26]. It should be noted that for the zero-sequence filter, it is mandatory to correctly (according to the manufacturer's recommendations) connect the neutral point of the phase capacitors Y: to ground or to the DC link buses of the FC (without this, there will be no effective suppression of common-mode components of the voltage).

Based on the use of SF for suppressing antiphase voltage components [6], the dominance of three-phase inductive reactors with a three-legged magnetic core in SF designs is quite understandable - their weight and size parameters are minimal. In [27], [28], the paths of closing the zero-sequence magnetic fluxes in three-phase inductive reactors with different designs of magnetic cores are shown. The three-legged core is the only one in which the zero-sequence magnetic fluxes of the phases are forced to close in the air. This feature leads to a very low zero-sequence impedance. Zero-sequence currents are not limited, zero-sequence voltages are not suppressed.

Therefore, in order to give the SF the properties of blocking the path of zero-sequence currents and suppressing common-mode voltages, it is advisable to use other designs of the inductive reactor magnetic core as part of the SF instead of the three-legged design: bank of three single-phase reactors, four-legged, five-legged [29], [30].

5 Conclusion

The circumstances considered in the article show that despite the good knowledge and widespread use of SF, in each specific case of their use it is necessary to carefully analyze the details of the characteristics of the load, the FC and the selected SF in order to best ensure the electromagnetic compatibility of the devices and avoid unwanted effects.

References:

[1] Cacciato M., Scarcella G., Scelba G., Spanik P., Sine Wave Filters Design for AC Motor Drives with Genetic Algorithms, *Communications - Scientific Letters of the University of Zilina*, Vol. 17, No. 11, 2015, pp. 102-109. 10.26552/com.C.2015.1A.102-109. https://doi.org/10.17073/2500-0632-2024-01-198.

[2] Baek S., Choi D., Bu H., Cho Y., Analysis and Design of a Sine Wave Filter for GaN-Based Low-Voltage Variable Frequency Drives, *Electronics*, Vol. 9, No. 345, 2020, pp. 1-12. https://doi.org/10.3390/electronics9020345.

[3] Pustovetov M., Experience in the Development of the Sine-Wave Filter for High-Power Variable Voltage Variable Frequency Drive with Medium Voltage Induction Motor, *WSEAS Transactions on Circuits and Systems*, Vol. 23, 2024, pp. 223-238, https://doi.org/10.37394/23201.2024.23.23.

[4] Petrov V.L., Pichuev A.V., Assessing the efficiency of measures to enhance electric power quality in variable-frequency drive for scraper conveyors, *Gornye nauki i tekhnologii = Mining Science and Technology (Russia)*, Vol. 9 (1), 2024, pp. 60-69. https://doi.org/10.17073/2500-0632-2024-01-198.

[5] Shchurov N.I., Myatezh S.V., Lisitsyn P.S., Abramov E.Yu., Latyshev R.N., Reducing the Harmonics Level in a Three-Level Single-Phase Autonomous Inverter without Pulse-Width Modulation, *Russian Electrical Engineering*, Vol. 95, No. 5, 2024, pp. 402-411. https://doi.org/10.3103/S1068371224700445.

[6] IEC/TS 61800-8. Technical Specification. *Adjustable speed electrical power drive systems – Part 8: Specification of voltage on the power interface*, Moscow.

[7] Danfoss. Output Filters Design Guide, [Online]. https://www.rpmecatronica.com/system/storage/download/130B2447.pdf?key=GG48eKtcD68412CiJv4wXIE4dD8zpzLZ (Accessed Date: May 15, 2025).

[8] Data Sheet. Sine Wave Filters FN5420. Schaffner, [Online]. https://www.schaffner.com/product/FN5420/Schaffner_datasheet_FN5420.pdf (Accessed Date: May 15, 2025).

[9] Tauscher Transformatoren. Sinusoidal filter, motor filters, three-phase – 4 kHz, [Online]. https://www.tauscher-transformatoren.de/assets/pdf/D_21_23.pdf (Accessed Date: May 15, 2025).

[10] Varsha Shah, Nargis Shaikh, Ramkumar Maurya, Sudesh Agrawal, Chandramohan Konduri, Arun Kumar Mishra, Vikas Dubey, LC Filter Design for Sine PWM Inverter Using Voltage Drop Across Inductor Technique, *Journal of Engineering Science*, Vol. 11, Iss. 6, 2020, pp. 856-859, [Online]. https://jespublication.com/upload/2020-1106126.pdf (Accessed Date: May 15, 2025).

[11] Kolpakhchyan P.G., Lobov B.N., Ali Dzhurni Al Madjid Rahgat, Mathematical Modeling of Stand-Alone Inverters Voltage, *Izvestiya Vysshikh Uchebnykh Zavedenii. Elektromekhanika. (Russian Electromechanics)*, No. 4(540), 2015, pp. 38-41.

[12] Brown M, *Power supply cookbook*, 2nd ed., Boston: Newnes, 2001, 265 p.

[13] IEC 61000-4-7. International Standard. *Electromagnetic compatibility (EMC) – Part 4-7: Testing and measurement techniques – General guide on harmonics and interharmonics measurements and instrumentation, for power supply systems and equipment connected thereto*.

[14] Binder A., *Motor Development for Electrical Drive Systems*, Germany: Technische universitat Darmstadt. Institut für Elektrische Energiewandlung, iss. SS 2017, 149 p. [Online]. Available: https://www.ew.tu-darmstadt.de/media/ew/rd/ew_vorlesungen/lv_md/Text_book.pdf (Accessed Date: March 16, 2025).

[15] Song-Manguelle J., Ekemb G., Mon-Nzongo D.L., Jin T., Doumbia M.L., A Theoretical Analysis of Pulsating Torque Components in AC Machines With Variable Frequency Drives and Dynamic Mechanical Loads, *IEEE Transactions on Industrial Electronics*, Vol. 65, No. 12, 2018, pp. 9311–9324. https://doi.org/10.1109/TIE.2018.2823681.

[16] IEC 60076-1. International Standard. *Power transformers – Part 1: General.*

[17] Pustovetov M., “Determining the Parameters of the Sine-Wave Filter. Factors Affecting Filtration Quality, *Journal of Engineering Research and Sciences*, Vol. 1, No. 4, 2022, pp. 127–136. https://doi.org/10.55708/js0104015.

[18] Datasheet. Sine wave filters FN 5040 HV, [Online]. https://www.verical.com/datasheet/schaffner-emc-sinusoidal-output-filter-fn-5040hv-28-84-7366962.pdf (Accessed Date: March 16, 2025).

[19] Schwab A.J., Kürner W., *Elektromagnetische Verträglichkeit*, 6th ed., Berlin, Heidelberg: Springer, 2011, 545 p. https://doi.org/10.1007/978-3-642-16610-5.

[20] Vostrov K., Pyrhönen J., Ahola J., "Shielding the end windings to reduce bearing currents," *2020 International Conference on Electrical Machines (ICEM)*, Gothenburg, Sweden, 2020, pp. 1431-1437,

https://doi.org/10.1109/ICEM49940.2020.9270673.

[21] Litovchenko V.V., Pudovikov O.E., Nazarov D.V., Rotanov V.N., Sharov V.A., High-Frequency Common-Mode Voltage as a Cause of Damage to the Bearings of Traction Motors, *Russian Electrical Engineering*, Vol. 95, No. 9, 2024, pp. 748-756. https://doi.org/10.3103/S1068371224700949.

[22] Turzy´nski M., Musznicki P., A Review of Reduction Methods of Impact of Common-Mode Voltage on Electric Drives, *Energies*, Vol. 14, 2021, p. 4003. https://doi.org/10.3390/en14134003.

[23] Pastura M., Nuzzo S., Kohler M., Barater D., "Dv/Dt Filtering Techniques for Electric Drives: Review and Challenges," *IECON 2019 - 45th Annual Conference of the IEEE Industrial Electronics Society*, Lisbon, Portugal, 2019, pp. 7088-7093, https://doi.org/ 10.1109/IECON.2019.8926663.

[24] M.Y. Pustovetov, Voinash S.A., "Analysis of dv/dt Filter Parameters Influence on its Characteristics. Filter Simulation Features," *2019 International Conference on Industrial Engineering, Applications and Manufacturing (ICIEAM)*, Sochi, Russia, 2019, pp. 1-5, https://doi.org/10.1109/ICIEAM.2019.8743007

[25] TDK. EMC filters. 3-line sine-wave EMC output filters SineFormer 520 V AC, 6 A ... 320 A, 40 °C, [Online]. https://www.tdk-electronics.tdk.com/inf/30/db/emc_2014/B84143V_R127.pdf (Accessed Date: March 16, 2025).

[26] Tallam R.M., Skibinski G.L., Shudarek T.A., Lukaszewski R.A., "Integrated differential-mode and common-mode filter to mitigate the effects of long motor leads on AC drives," *2010 IEEE Energy Conversion Congress and Exposition*, Atlanta, GA, USA, 2010, pp. 838-845, doi: 10.1109/ECCE.2010.5617910.

[27] Jiang, Y., Li, J., Pan, S., Zhang, X., Hu, P., Zhang, H., Research on the Comparison Analyses of Three-Phase Discrete and Integrated LC Filters in Three-Phase PV Inverter, *International Journal of Photoenergy. Special Issue Photovoltaic Materials and Devices*, Vol. 2013, 2013, pp. 1-14, Article ID 217023. https://doi.org/10.1155/2013/217023.

[28] Song J.S., Kim J.S., Cho G.J., Kim C.H., Cho N.H., "A Study on Zero Sequence Impedance of 3-limb Core Transformer," *2019 IEEE PES GTD Grand International Conference and Exposition Asia (GTD Asia)*, Bangkok, Thailand, 2019, pp. 559-564, https://doi.org/10.1109/GTDAsia.2019.8716026.

[29] Owzareck M., Froehling S., Langfermann S., Fraeger L., Parspour N., "Calculation Method for Four-Legged Inductors of Sine-Wave Filters in Drive Systems," *PCIM Europe digital days 2021 - International Exhibition and Conference for Power Electronics, Intelligent Motion, Renewable Energy and Energy Management*, Frankfurt, Germany, 2021, pp. 1-8. [Online]. https://www.vde-verlag.de/proceedings-en/565515248.html (Accessed Date: March 16, 2025).

[30] Four leg choke for common-mode rejection, [Online]. https://www.schmidbauer.net/en/products/four-leg-choke/ (Accessed Date: March 16, 2025).

Contribution of Individual Authors to the Creation of a Scientific Article (Ghostwriting Policy)

The author equally contributed to the present research, at all stages from the formulation of the problem to the final findings and solution.

Sources of Funding for Research Presented in a Scientific Article or Scientific Article Itself

No funding was received for conducting this study.

Conflict of Interest

The author have no conflicts of interest to declare that are relevant to the content of this article.